Photomedicine and Laser Surgery
Volume 32, Number 10, 2014

Pp. 561–573
DOI: 10.1089/pho.2014.3749

The Biological Effects of Quadripolar Radiofrequency Sequential Application: A Human Experimental Study

Giovanni Nicoletti, MD, FEBoPRAS,[1–3] Antonia Icaro Cornaglia, ScD, PhD,[2,4] Angela Faga, MD, FICS,[1–3] and Silvia Scevola, MD, PhD[2]

Abstract

Objective: An experimental study was conducted to assess the effectiveness and safety of an innovative quadripolar variable electrode configuration radiofrequency device with objective measurements in an *ex vivo* and *in vivo* human experimental model. ***Background data:*** Nonablative radiofrequency applications are well-established anti-ageing procedures for cosmetic skin tightening. ***Methods:*** The study was performed in two steps: *ex vivo* and *in vivo* assessments. In the *ex vivo* assessments the radiofrequency applications were performed on human full-thickness skin and subcutaneous tissue specimens harvested during surgery for body contouring. In the *in vivo* assessments the applications were performed on two volunteer patients scheduled for body contouring surgery at the end of the study. The assessment methods were: clinical examination and medical photography, temperature measurement with thermal imaging scan, and light microscopy histological examination. ***Results:*** The *ex vivo* assessments allowed for identification of the effective safety range for human application. The *in vivo* assessments allowed for demonstration of the biological effects of sequential radiofrequency applications. After a course of radiofrequency applications, the collagen fibers underwent an immediate heat-induced rearrangement and were partially denaturated and progressively metabolized by the macrophages. An overall thickening and spatial rearrangement was appreciated both in the collagen and elastic fibers, the latter displaying a juvenile reticular pattern. A late onset in the macrophage activation after sequential radiofrequency applications was appreciated. ***Conclusions:*** Our data confirm the effectiveness of sequential radiofrequency applications in obtaining attenuation of the skin wrinkles by an overall skin tightening.

Introduction

Over the past decade, radiofrequency (RF) has become an important and frequently used technology in aesthetic medicine. The mechanism of action of RF is based on an oscillating electrical current (2,000,000–3,000,000 times/sec) forcing collisions between charged molecules and ions, which are then transformed into heat.[1] A further contribution to the increase in the local temperature is provided by the radiation component of the RF field, with electromagnetic energy transfer to the water-rich dermal matrix.

Noninvasive delivery of RF energy to collagen and subcutaneous tissues produces collagen remodelling, therefore, achieving noninvasive tightening of lax skin and body contouring.[2,3] RF-treated skin displays an immediate and temporary change in the helical structure of collagen, with fibrils showing a greater diameter than that of fibers pretreatment.[4]

It is also thought that RF thermal stimulation results in a microinflammatory stimulation of fibroblasts, which produces new collagen, new elastin, and other substances, to enhance dermal structure.[1,5]

The depth of penetration of RF energy is inversely proportional to the frequency. Consequently, lower frequencies of RF are able to penetrate more deeply. The currently available devices work with frequencies within the 1 Hz to 40.68 MHz range.

Two different forms of RF delivery have been developed so far: monopolar and bipolar. Monopolar systems deliver current through a single contact electrode with an

[1]Plastic and Reconstructive Surgery, Department of Clinical Surgical Diagnostic and Pediatric Sciences, University of Pavia, Pavia, Italy.
[2]Advanced Technologies for Regenerative Medicine and Inductive Surgery Research Center, University of Pavia, Pavia, Italy.
[3]Plastic and Reconstructive Surgery Unit, Salvatore Maugeri Research and Care Institute, Pavia, Italy.
[4]Histology and Embryology Unit, Department of Public Health, Neuroscience, Experimental and Forensic Medicine, University of Pavia, Pavia, Italy.

accompanying grounding pad that serves as a low resistance path for current flow to complete the electrical circuit; the active electrode concentrates most of the energy near the point of contact, and energy rapidly diminishes as the current flows through the body toward the grounding electrode. As a result, the tissue in the treated area is heated rather deeply (usually up to 20 mm) and intensely.[2]

Bipolar devices pass electrical current between two electrodes closely positioned to the skin; no grounding pad is necessary with these systems because no current flows throughout the rest of the body. The depth of penetration is approximately half the distance between the two electrodes.[3]

As a result, the tissue in the treated area is heated less deeply (usually up to 2–4 mm in depth) and less intensely than with the monopolar RF devices.[6]

Despite its lesser absolute effectiveness, the bipolar technology is currently gaining an increasing popularity, as it allows fair outcomes with significantly less invasive applications.[7]

Nowadays, patients asking for cosmetic medical treatments expect perfect results, with a minimum of work and social downtime. Therefore, such innovative noninvasive treatments have been progressively replacing the traditional and time-honored surgical procedures for skin tightening.

The increasingly large number of technological innovations proposed on the global market require rigorous study protocols for the assessment of safety and effectiveness prior to authorization for human use. As a group of academic plastic surgeons actively involved in aesthetic surgery and medicine research, we were commissioned to assess the effectiveness and safety of an innovative quadripolar variable electrode configuration RF device.

Materials and Methods

The study was conducted at the Advanced Technologies for Regenerative Medicine and Inductive Surgery Research Center of the University of Pavia, Italy, in cooperation with the Plastic and Reconstructive Surgery Unit of the Salvatore Maugeri Research and Care Institute, Pavia, Italy, and the Histology and Embryology Unit, Department of Public Health, Neuroscience, Experimental and Forensic Medicine, University of Pavia, Pavia, Italy.

The study was approved by the University of Pavia Ethical Committee. A formal informed written consent was obtained from all of the patients and the study conformed to the Declaration of Helsinki.

A novel Class I RF generator, RADIO4™, produced by Novavision Group s.p.a., (Via dei Guasti 29, 20826 Misinto, Milan, Italy) was tested. RADIO4 is based on a four electrode system with software-controlled automatic dynamic configuration providing a 1 MHz RF current circulation. The variable electrode configuration allows for creation of custom-made electric fields promoting thermal energy transfer to the tissue from RF current circulation. The device allows three possible electrode configurations within the four electrodes (Fig. 1):

- 1–3: one transmitter electrode and three receiver electrodes
- 2×2: two transmitter electrodes and two receiver electrodes in a cross fashion

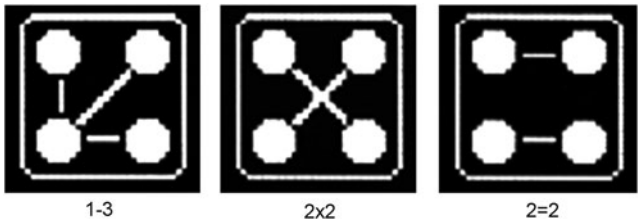

FIG. 1. The three electrode configuration options in the tested device: (1) 1–3, one transmitter electrode and three receiver electrodes; (2) 2×2, two transmitter electrodes and two receiver electrodes in a cross fashion; (3) 2=2, two transmitter electrodes and two receiver electrodes in a parallel fashion.

- 2=2: two transmitter electrodes and two receiver electrodes in a parallel fashion

The single electrode configuration is allowed to swap over at a time interval adjustable between 1 and 9 sec.

The maximum device working power is 55 W adjustable within a 5–100% delivery range. The device is equipped with an original patented safety technology, Radiofrequency Safety System (RSS™), and has been developed for noninvasive treatment of skin wrinkles and cellulite and for skin tightening.

The study was performed in two steps: *ex vivo* and *in vivo* assessments.

Ex vivo assessment

The ex vivo assessment was conducted on eight human anatomical specimens, including full thickness skin and subcutaneous tissue harvested from four female patients during sessions of abdominoplasty. The specimens underwent the experimental process after surgical harvesting, and the average time delay between harvesting the tissue and starting the experiment was 10 min. The tests were conducted in a dedicated air conditioned room at a temperature of 23°C. A control biopsy, including full thickness skin and adipose tissue, was harvested from each specimen before treatment.

FIG. 2. *Ex vivo* radiofrequency application with the device's probe.

FIG. 3. Areas of abdominal fat that were investigated on the two patients scheduled for abdominoplasty.

The effects of RFs on the specimens were assessed with the association of three different methods:

- Clinical full examination and medical photography
- Temperature measurement in the specimens before and after the treatments with thermal imaging scan using the AVIO Thermal Video System TVS 500 camera with an uncooled infrared sensor with a 8–14 μm spectrum sensitivity, 320 × 240 pixel thermal image resolution, and 0.1°C thermal resolution (Nippon Avionics Co., Ltd. Gotanda Kowa Bldg., 1–5, Nishi-Gotanda 8-chome, Shinagawa-ku, Tokyo, 141-0031 Japan).
- Histological examination at light microscopy. Tissue samples were fixed in a 4% paraformaldehyde solution in phosphate buffer for 6 h, cryoprotected by immersion in sucrose saturated solution, frozen in liquid nitrogen, and finally cut in a cryostat. Finally, tissue sections were routinely stained using hematoxylin and eosin.

A water gel was applied on the skin surface in order to allow an optimal delivery of the RFs from the probe to the tissues (Fig. 2). The gel was stored at room temperature (23°C).

The study was performed using the 1–3 electrode configuration modality, Radio Frequency System (RFS) 1–3, and the configuration swap over time (RFS time) was set at 5 sec.

The eight specimens were divided into four groups of two and the RF was delivered to each group at the following percentages of the maximum device working power: 25% (13.75 W), 50% (27.50 W), 75% (41.25 W), and 100% (55 W). The energy was delivered in continuous mode (duty cycle 100%, time on = 1.000 msec, time off = 0 msec). The scheduled maximum application time was 4 min. As the specimens treated with the maximum device working power displayed clinical evidence of full thickness burn after few seconds, the applications in this group were discontinued at this time.

At the end of the application, a full thickness skin and subcutaneous tissue biopsy was harvested in each specimen from the site of maximum tissue warming, as displayed by the thermocamera scan.

In vivo assessment

The *in vivo* investigations were conducted on two volunteer female patients scheduled for abdominoplasty at the end of the experimental study (Fig. 3). The assessments

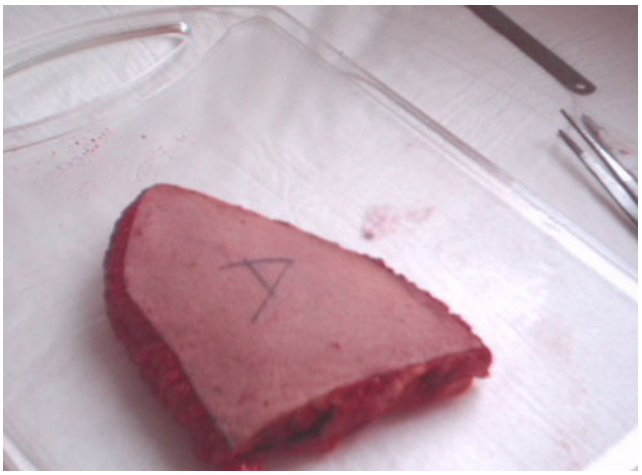

FIG. 4. Human *ex vivo* specimen before treatment: macroscopic view.

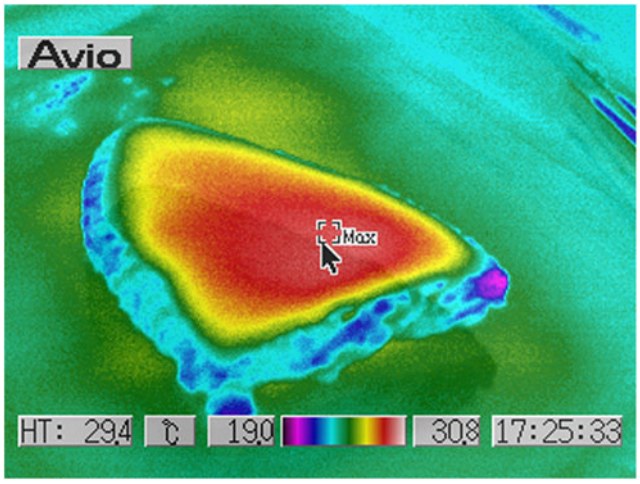

FIG. 5. Human *ex vivo* specimen before treatment: thermal imaging scan.

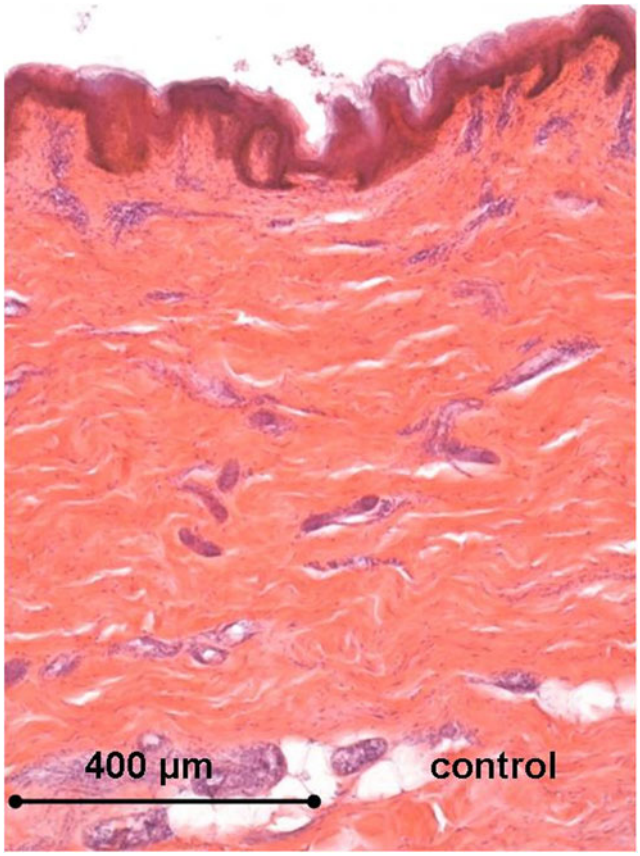

FIG. 6. Histology of the human *ex vivo* specimen before treatment: the epidermis displays a regular multilayered structure, the dermis shows regular dermal papillae with thin collagen fibers and thick collagen bundles in the reticular dermis. Light microscopy, hematoxylin and eosin staining, bar 400 μm.

were performed on the lower abdominal skin area bounded above by the umbilicus, below by the pubis, and on each side by the anterior superior iliac spine. The applications were performed in the same dedicated air conditioned room at a temperature of 23°C, as in the *ex vivo* tests.

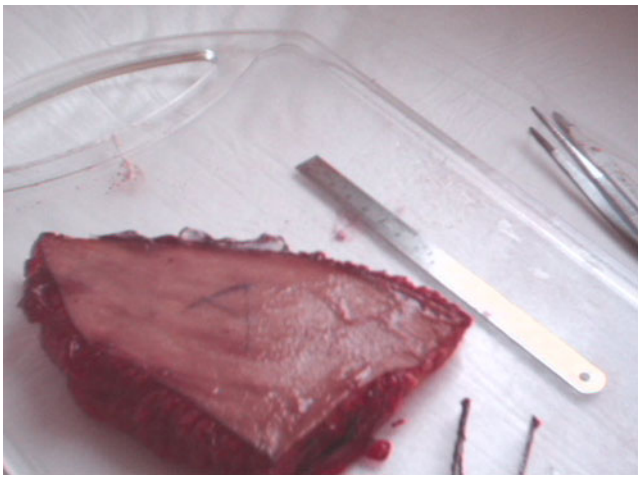

FIG. 7. Human *ex vivo* specimen after treatment with 25% of the maximum device working power (13.75 W): macroscopic view.

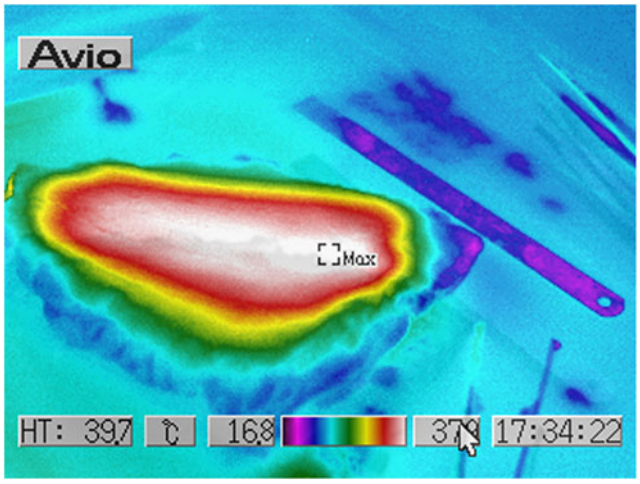

FIG. 8. Human *ex vivo* specimen after treatment with 25% of the maximum device working power (13.75 W): thermal imaging scan.

A control biopsy, including full thickness skin and adipose tissue, was harvested before the treatment. Three sequential treatments were performed with 2 weeks' interval. A water gel was applied on the skin surface in order to allow an optimal RF energy delivery from the probe to the tissues.

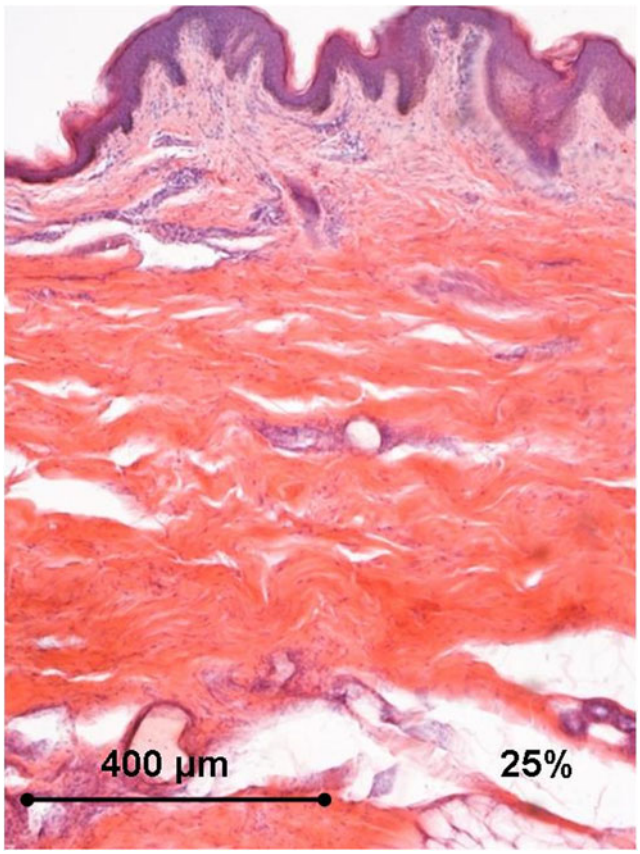

FIG. 9. Histology of the human *ex vivo* specimen after treatment with 25% of the maximum device working power (13.75 W): complete sparing of the epidermis that displays normal structure; an early thickening of the collagen bundles is appreciated in the deep dermal layers. Light microscopy, hematoxylin and eosin staining, bar 400 μm.

FIG. 10. Histology of the human *ex vivo* specimen after treatment with 25% of the maximum device working power (13.75 W): the sweat glands and the nerves (asterisk) display a normal structure and a regular staining. Light microscopy, hematoxylin and eosin staining, bar 40 μm.

The applied parameters were the same as in the *ex vivo* section of the study: RFS 1–3, duty cycle 100%, RFS time 5 sec.

Three sequential treatments were scheduled with 2 weeks' interval. Each treatment lasted 20 min.

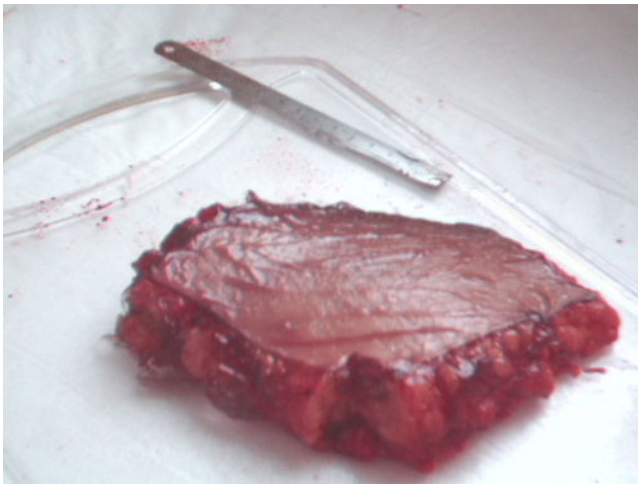

FIG. 11. Human *ex vivo* specimen after treatment with 50% of the maximum device working power (27.50 W): macroscopic view.

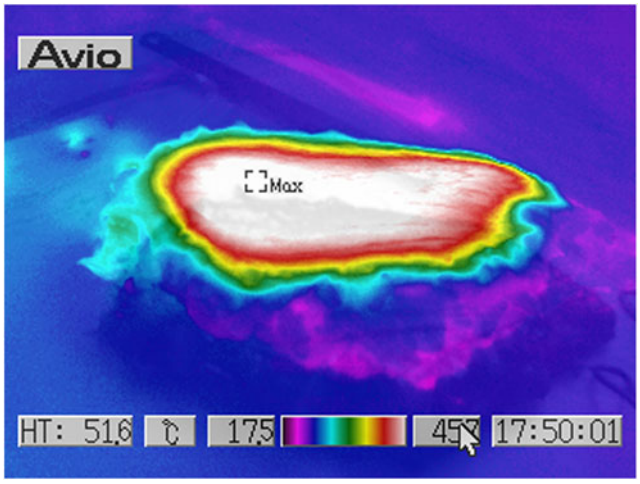

FIG. 12. Human *ex vivo* specimen after treatment with 50% of the maximum device working power (27.50 W): thermal imaging scan.

The initial working power was 45% (24.75 W); however, following a patient's consistent subjectively perceived discomfort, the energy delivery power was reduced to 35–40% (19.25–22 W) in all of the tests, and this level was comfortably tolerated. On occasion of the second treatment in

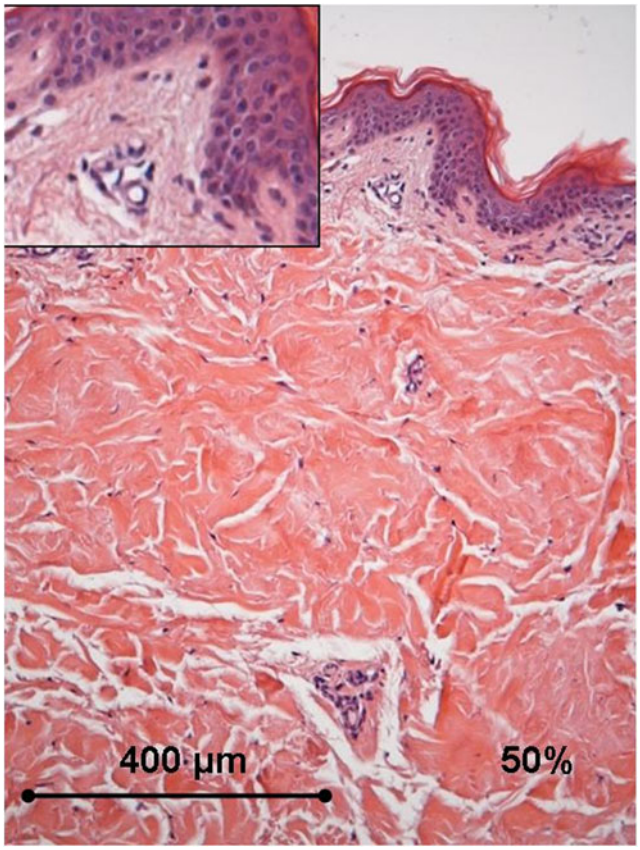

FIG. 13. Histology of the human *ex vivo* specimen after treatment with 50% of the maximum device working power (27.50 W): the thickening of the collagen fibers in the papillary dermis is appreciated, whereas the blood vessels in the dermal papillae do not display any alteration (box). Light microscopy, hematoxylin and eosin staining, bar 400 μm.

FIG. 14. Histology of the human *ex vivo* specimen after treatment with 50% of the maximum device working power (27.50 W): the sweat glands and the nerves (asterisk) display a normal structure and a regular staining. Light microscopy, hematoxylin and eosin staining, bar 40 μm.

one patient, the energy delivery power had to be reduced to 20% (11 W) in the last 8 min of application, because of severe subjective discomfort.

The effects of the RF applications on the patient were assessed with the same methods used in the *ex vivo* as-

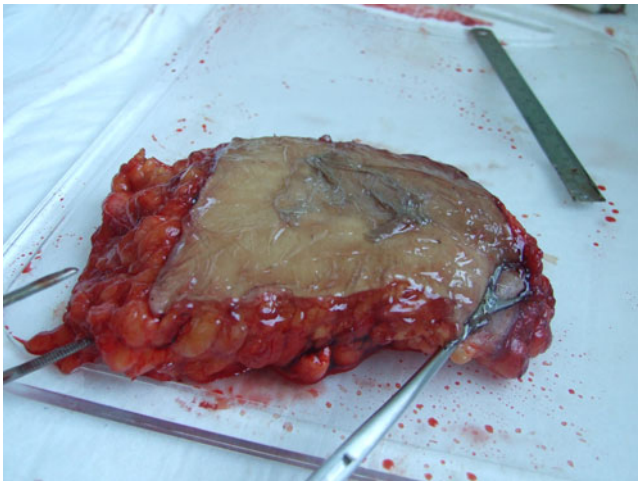

FIG. 15. Human *ex vivo* specimen after treatment with 75% of the maximum device working power (41.25 W): macroscopic view.

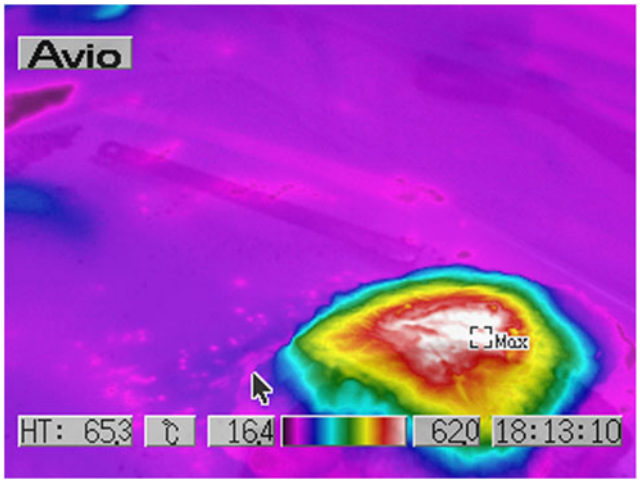

FIG. 16. Human *ex vivo* specimen after treatment with 75% of the maximum device working power (41.25 W): thermal imaging scan.

sessment: clinical examination, thermocamera scan, and histological examination of treated tissue biopsies. Three punch full thickness skin and subcutaneous tissue biopsies were harvested from each treated area. The first biopsy was harvested 2 weeks after the first treatment, the second one 2

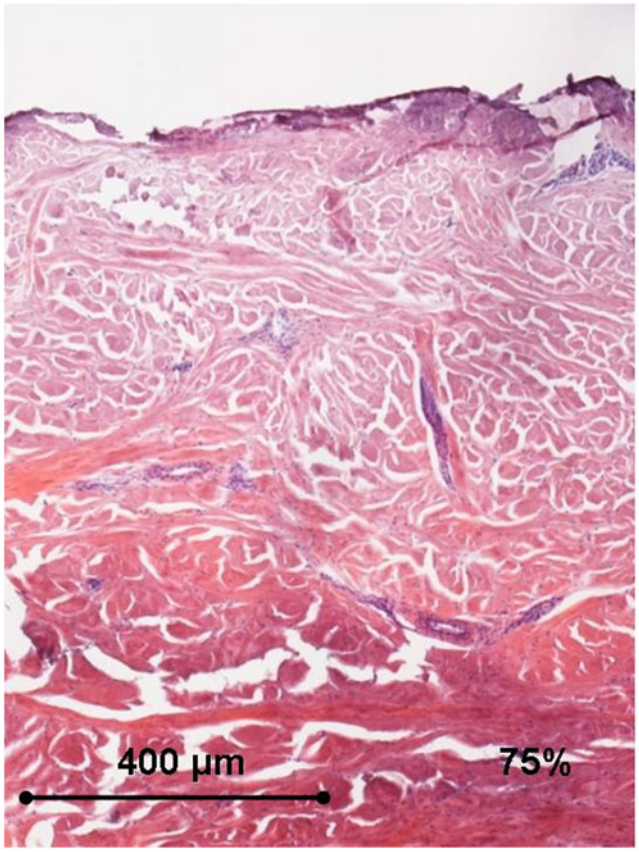

FIG. 17. Histology of the human *ex vivo* specimen after treatment with 75% of the maximum device working power (41.25 W): the epidermis is necrotic, and the collagen bundles display a remarkable diffuse thickening in the whole dermis. Light microscopy, hematoxylin and eosin staining, bar 400 μm.

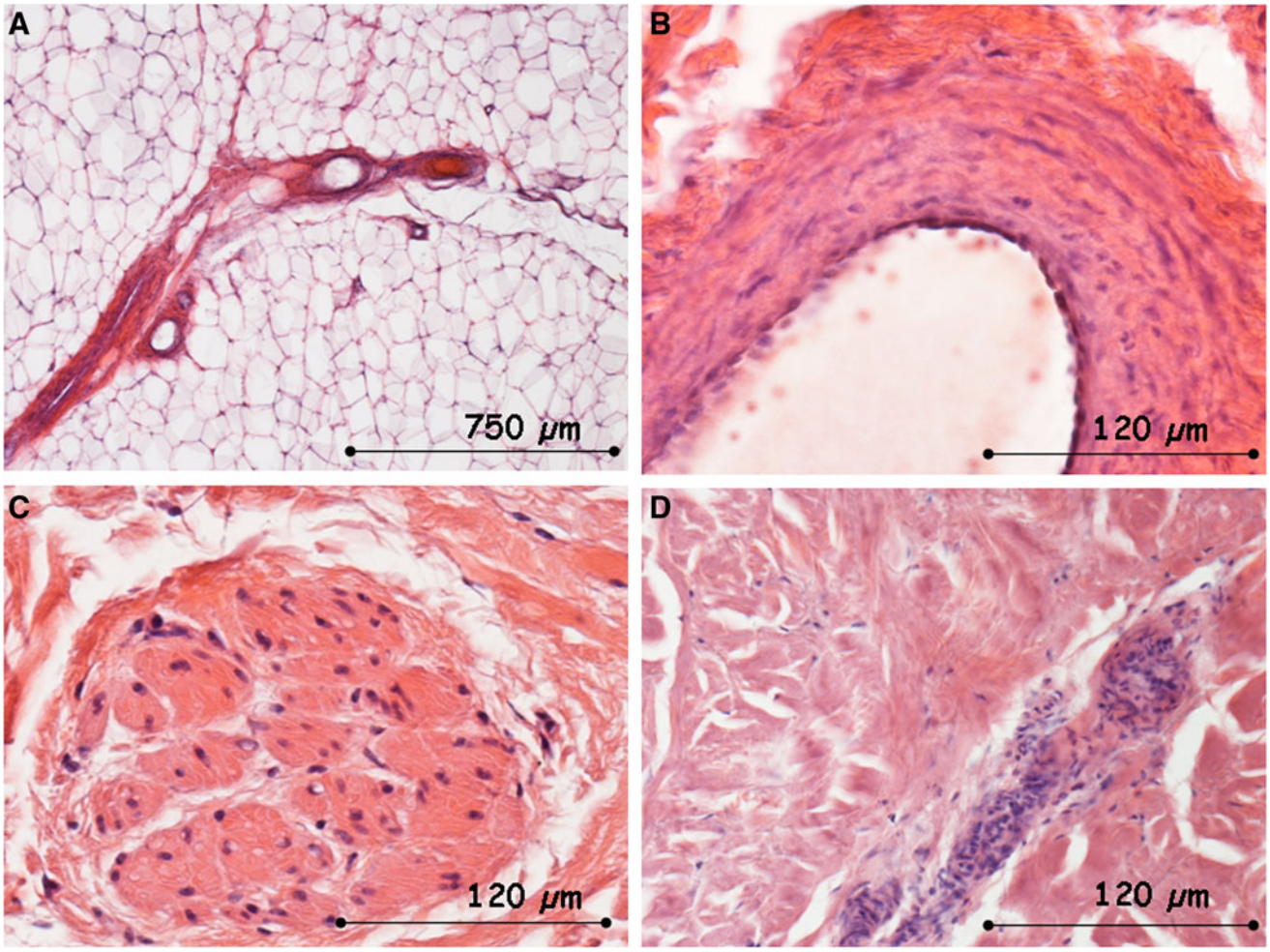

FIG. 18. Histology of the human *ex vivo* specimen after treatment with 75% of the maximum device working power (41.25 W): the subcutaneous tissue (**A**, bar 750 μm), the vascular wall with its endothelial lining (**B**, bar 120 μm), the nerves (**C**, bar 120 μm), and the sweat glands (**D**, bar 120 μm) appear intact. Light microscopy, hematoxylin and eosin staining.

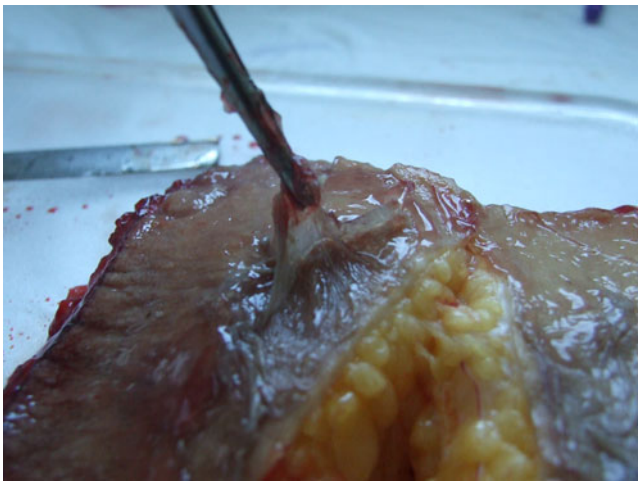

FIG. 19. Human *ex vivo* specimen after treatment with 100% of the maximum device working power (55 W): macroscopic view; after a few seconds of application, the epidermis displays separation from the dermis, and the subcutaneous tissue shows coagulative necrosis in the superficial layer while it appears intact in the deep layer.

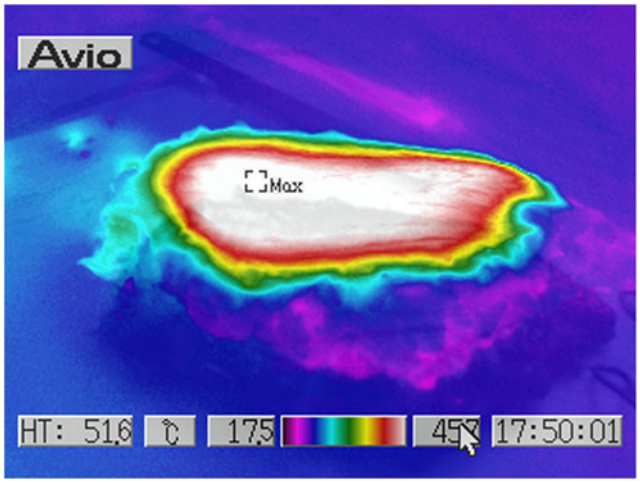

FIG. 20. Human *ex vivo* specimen after treatment with 100% of the maximum device working power (55 W): thermal imaging scan.

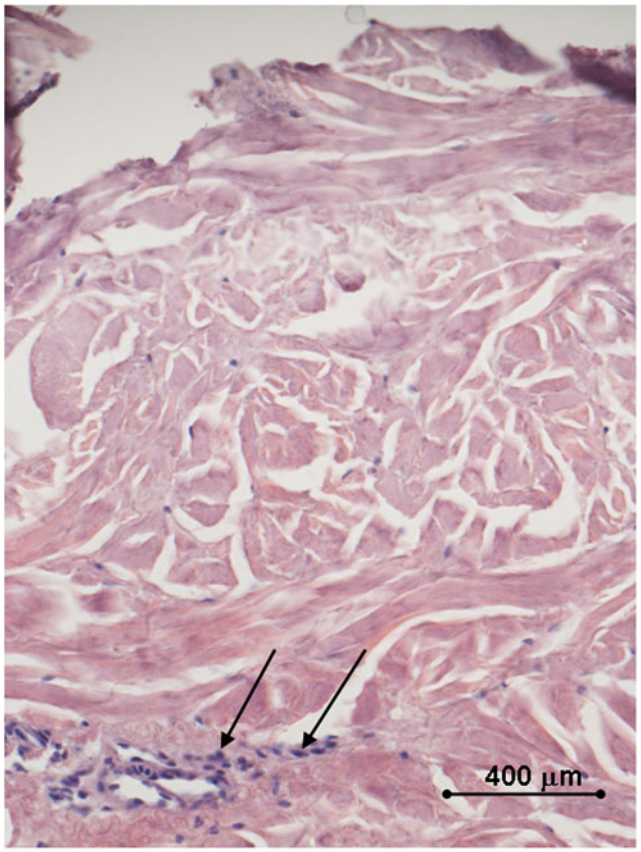

FIG. 21. Histology of the human *ex vivo* specimen after treatment with 100% of the maximum device working power (55 W): a complete loss of the epidermal lining and a massive coagulative dermal necrosis are appreciated; the sweat glands display early signs of necrosis (arrows). Light microscopy, hematoxylin and eosin staining, bar 400 μm.

weeks after the second treatment, and the third one 10 weeks after the last treatment.

Results

Ex vivo assessment (Figs. 4–21)

Clinical examination. At the end of the application, the specimen treated with 25% of the maximum working power did not display any macroscopic skin surface alterations, although the subcutaneous tissue was softer at palpation and displayed some degree of shrinkage.

The specimen treated with 50% of the maximum working power showed a significant wizening of the subcutaneous tissue after 90 sec, whereas the skin showed a remarkable retraction and separation from the subcutaneous tissue in 3 min; after 4 min, the overall appearance was as a deep skin and subcutaneous tissue burn.

The specimen treated with 75% of the maximum working power displayed a total skin retraction and separation from the subcutaneous tissue after 90 sec, with coagulative necrosis of the subcutaneous fat.

The specimen treated with full working power displayed a full thickness burn appearance in a few seconds.

Temperature report. The energy application was followed by an increase of the specimen temperature proportional to the application power and time, with a gradient decreasing from the surface to the subcutaneous adipose tissue (Table 1).

Histological examination. All of the specimens displayed scattering of the collagen bundles that was appreciated from the papillary dermis up to 1.5 cm in depth. Such an alteration was proportional to both time and energy power application. The epithelial superficial lining appeared intact up to the application of 50% of the maximum working power. The subcutaneous tissue, the nerves, and the skin glands appeared intact up to the application of 75% of the maximum working power.

In vivo assessment

Clinical examination. The treatments were well tolerated, and the patients occasionally referred to tolerable local heat sensation, burning pain, and electric shock sensation. At the end of the treatments, no skin lesions were appreciated. After two applications, the patients referred to improved local skin softness and smoothness.

Temperature report. The energy application was constantly followed by an increase of the skin surface temperature (Table 2, Fig. 22).

Histological examination (Figs. 23–29). The *in vivo* findings 2 weeks after the first treatment closely resemble those in the *ex vivo* specimens: the collagen bundles appeared diffusely scattered whereas the epithelial superficial lining, the subcutaneous tissue, the nerves, and the skin glands appeared intact.

Two weeks after the second application, the collagen bundles appeared coagulated in small grumes in the papillary dermis and in larger grumes in the underlying reticular dermis. The epidermis appeared normal. The overall connective cell count and general pattern did not differ from the

TABLE 1. AVERAGE *EX VIVO* SPECIMEN TEMPERATURE VALUES MEASURED AT DIFFERENT WORKING POWER APPLICATIONS

	T pre	*T post 4' 25%*	*T post 4' 50%*	*T post 4' 75%*	*T post 45'' 100%*
Skin surface	25.8°	37°Δ + 11.2°	47.7°Δ + 21.9°	55 Δ + 29.2°	60 Δ + 34.2°
Subcutaneous adipose tissue	27.5°	28.8°Δ + 1.3°	27.5°Δ 0	27.2 Δ − 0.3°	27 Δ − 0.5°

T, temperature in degrees Celsius; Δ, average temperature delta between pre- and post-treatment; ', minutes; '', seconds.

Table 2. Average Skin Surface Temperature Values Measured at the End of the *In Vivo* Treatment

	T pre	*T post*	Δ
Skin surface	29.6°	38.2°	+8.6°

T, temperature in degrees Celsius; Δ, average temperature delta between pre- and post-treatment.

control areas. A remarkable thickening in the elastic fibers with a regular reticular pattern and a definite orientation perpendicular to the basal membrane in the papillary dermis was appreciated in the treated areas versus the controls.

Ten weeks after the third application, the macrophages had moved from the perivascular niche and displayed a slight increase in their count, thus suggesting some sort of functional activation. Such a finding suggests the presence of coagulated collagen fragments and/or other tissue debris.

Discussion

The device used in our study is one of the innovative multipolar developments of the bipolar technology.[8]

As any technical innovation should undergo a rigorous assessment of both safety and effectiveness prior to clinical use, our study provided a prudent design with two different and sequential steps.

The *ex vivo* experimental assessments allowed for identification of the effective safety range for human application, which was established between 11 and 22 W.

We deliberately opted for a random choice of only one electrode configuration out of three potentially available in the device setting, as the rigorous compliance requirements substantially limited the number of patients recruited for the study.

As expected, the biological effects of RF application were related to the thermal energy transfer to the tissues, and were proportional to both local temperature and exposure time.[9] All of the possible typical macro- and microscopic tissue burn features were observed in the *ex vivo* samples in relation to the different levels of applied energy. However, these effects were mainly appreciated in the dermis and subcutaneous tissue, with involvement of the overlying epidermis only for the highest applied energy levels. Such a figure is a peculiar advantage of RF technology that allows selective heat transfer to the dermis and subcutaneous tissue, yielding a controlled collagen alteration.

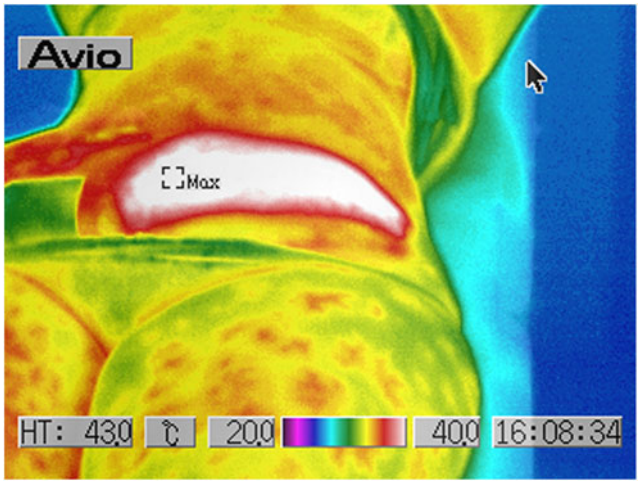

FIG. 22. Thermal imaging scan of the lower abdominal region after the *in vivo* treatment.

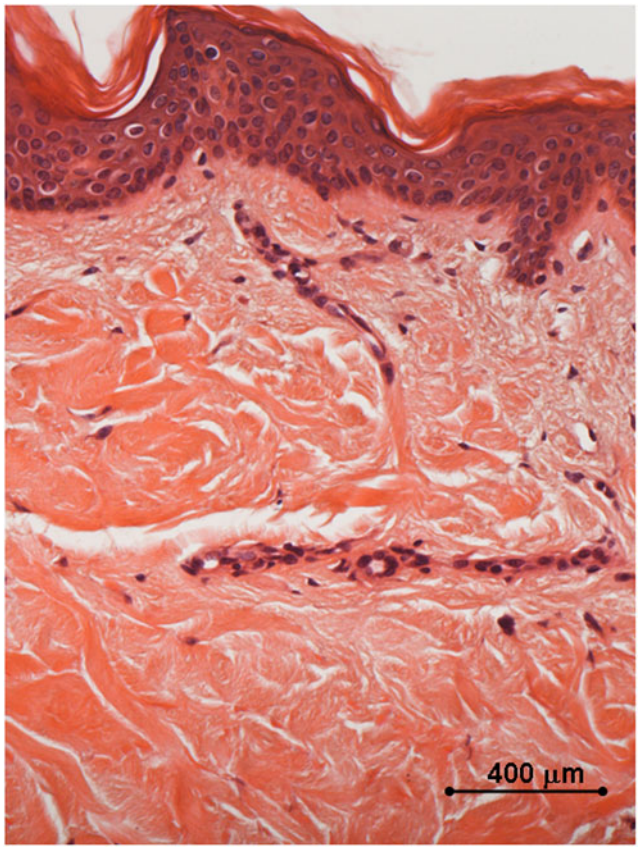

FIG. 23. Histology of *in vivo* control biopsy: the collagen fibers appear thin and outstretched. Light microscopy, hematoxylin and eosin staining, bar 400 µm.

After accurate definition of the effective safety range of RF applications on human tissues, the trial proceeded with the *in vivo* assessments.

These tests allowed for demonstration of the biological effects of the device under study at different time intervals.

The temperature changes reported in the *ex vivo* samples were partially compensated *in vivo* by the active thermoregulation and the local temperature increase was proportional to the application time.

A selective effect was appreciated in the more dense and compact tissues, as the dermis and the connective septa of the adipose tissue. The temperature reports and the histological examinations, both *ex vivo* and *in vivo*, consistently demonstrated selective scattering of the collagen bundles in the dermis. The small grumes observed in the reticular dermis of the *in vivo* samples 2 weeks after the second application might have followed local increase of RF current density in sites of enhanced electric conductivity with eventual focal temperature rise.

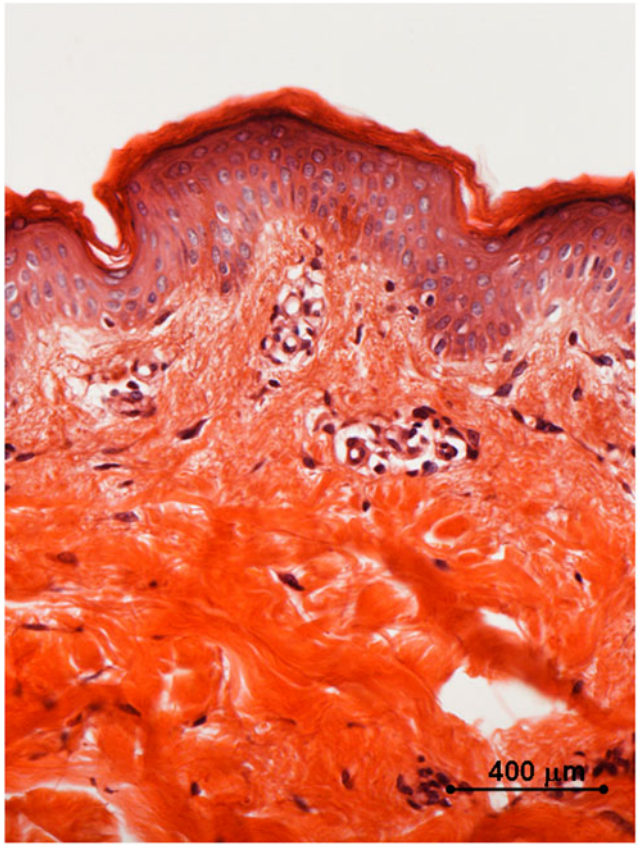

FIG. 24. Histology of *in vivo* sample harvested 2 weeks after the first treatment with 35–40% of the full device working power: early signs of coagulations are appreciated both in the papillary and in the reticular dermis. Light microscopy, hematoxylin and eosin staining, bar 400 μm.

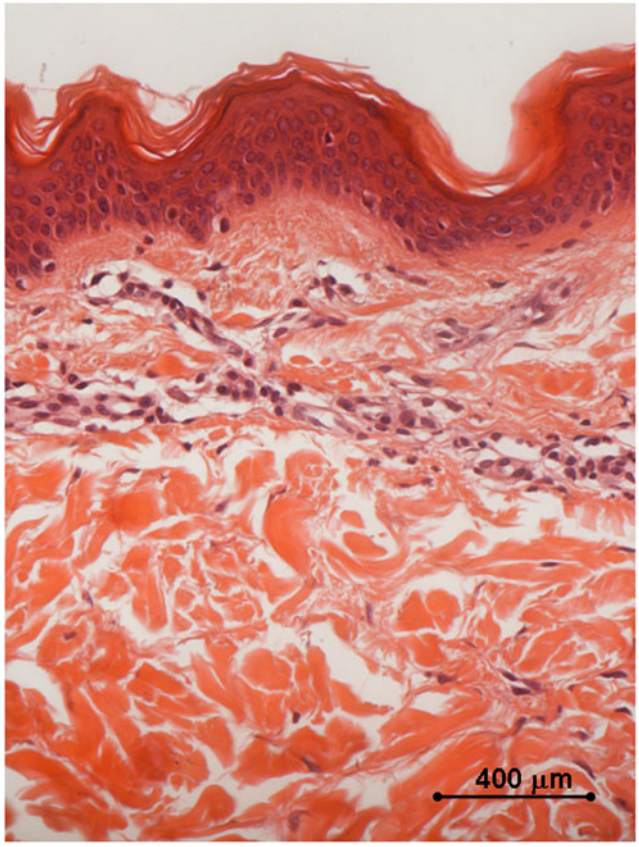

FIG. 25. Histology of *in vivo* sample harvested after two treatments with 35–40% of the full device working power, 1 month after the first treatment: the collagen fibers are coagulated in small grumes in the papillary dermis and in larger ones in the underlying layers; the epidermal lining is intact. Light microscopy, hematoxylin and eosin staining, bar 400 μm.

It is demonstrated that collagen fibers begin to curve at 52–55°C[10] and contract at 65°C,[11] and the denaturation threshold falls between 60° and 70°C.[12] According to the thermal imaging scan in our *ex vivo* and *in vivo* samples, such a temperature threshold was unlikely to have been approached, although it may be theoretically supposed that it occurred in very small and circumscribed tissue spots. We can, therefore, suppose that the observed structural changes of the collagen fibers were not related exclusively to the temperature rise.

The overall effects of the sequential *in vivo* RF applications observed on the connective fibers, both collagen and elastic, might suggest their spatial rearrangement in the absence of complete denaturation: actually, no signs of scarring were observed under the microscope in any of our samples. As the collagen and elastic fibers are highly hydrophobic and are invested by a highly electric conductive water rich matrix, they obviously tend to gather when the temperature in the investing highly hydrophilic matrix rises.

Some interesting changes were observed in the skin elastic fiber network after two sequential applications with 2 weeks' interval 1 month after the first treatment: the elastic fibers appeared thicker both in the papillary and the reticular dermis; however, although thick elastic fibers are a typical feature of skin photo- and chrono-ageing, in our samples their regular network pattern was found more similar to the juvenile one.

Such an interesting figure might also be explained by the shrinkage of the highly hydrophobic elastic fibers with exclusive physical mechanism after increase of the energetic potential in the local water rich environment. These data are consistent with the literature,[13] and are in favor of the bipolar technology, as the elastic fibers seem to significantly decrease after monopolar treatment. [2] The epidermis did not display any significant damage apart from a transient erythema at the end of the *in vivo* treatments.

Adipose tissue, endothelial cells, nerves, and skin adnexa appeared intact with power application up to 41.25 W (Figs. 10, 14, and 18). Such an evidence was consistent with the peculiar temperature gradient figure between the skin surface and the underlying adipose tissue where relevant temperature changes in the dermis were not transmitted to the underlying fat.

These data both confirmed the low thermal conductivity of the human skin and demonstrated the selective superficial distribution of the electromagnetic energy within the treated tissues.

The *in vivo* effects of the RF application included a slight macrophage activation after three sequential applications

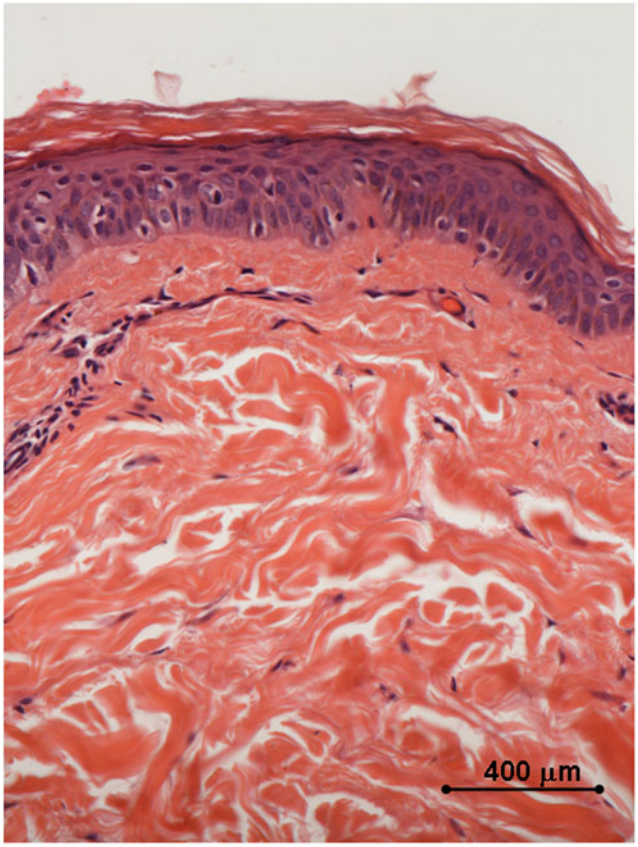

FIG. 26. Histology of *in vivo* sample harvested 10 weeks after the third treatment with 35–40% of the full device working power: the epidermis displays a normal differentiation and layer organization; a remarkable degree of collagen coagulation is appreciated in the papillary dermis, and the collagen bundles in the reticular dermis display a significant thickening as well. Light microscopy, hematoxylin and eosin staining, bar 400 μm.

with 2 weeks' interval, and might suggest the presence of tissue debris and/or coagulated collagen still being metabolized.

Nevertheless, no actual inflammatory cells or fibroblast response was appreciated.

However, a significant cellular response might be expected after further sequential applications, as suggested by the clinical protocols currently in use. The sequential application of RF for the treatment of skin wrinkling would definitely appear as a far different philosophy from the traditional surgical face and body lifting, as it would rely on a progressively induced and gently modulated body biological response. RF might, therefore, be considered an effective alternative for mild cases of skin laxity, and a useful completion of traditional surgical techniques.

Conclusions

The tested quadripolar variable electrode configuration RF equipment can provide selective and favorable changes in the dermal structure without side effects in the epidermis, vessels, and nerves when the energy delivery power ranges between 11 and 22 W.

After a course of RF application, the native collagen fibers underwent an immediate heat- induced rearrangement, and were just partially denaturated and progressively metabolized by the macrophages. Subsequently, an overall thickening and spatial rearrangement was appreciated both in the collagen and in the elastic fibers, the latter displaying a juvenile skin reticular pattern.

Our data demonstrated a late onset in the macrophage activation after sequential RF applications. It might be supposed that such a recruitment might be followed by a fibroblastic response at a later stage,[5] although such a hypothesis would suggest further investigations.

All of our data confirm the effectiveness of the RF applications in obtaining attenuation of the skin wrinkles by an overall skin tightening.

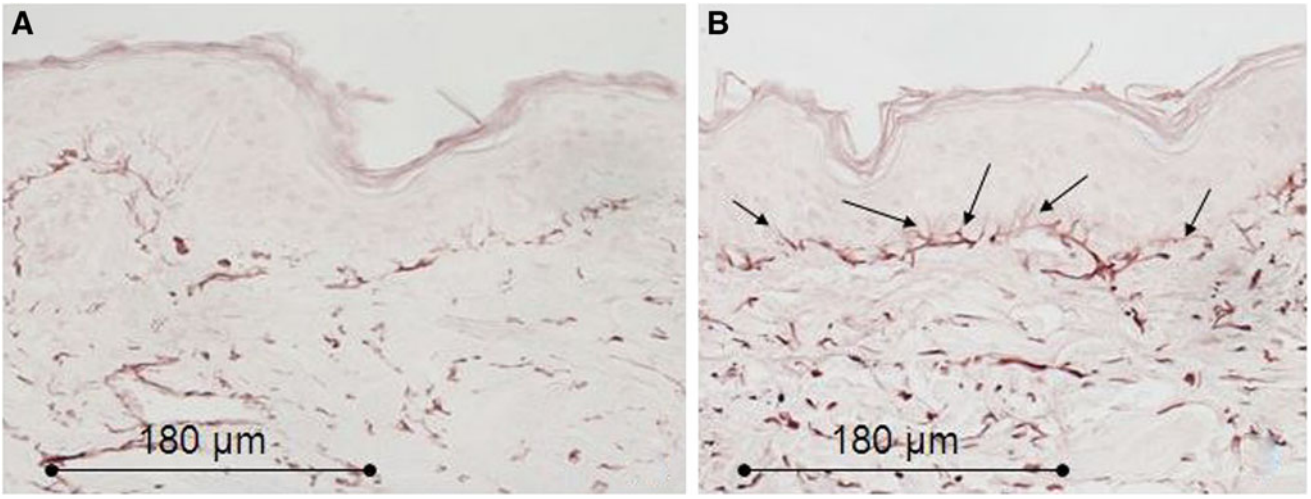

FIG. 27. Histology for elastic fibers of *in vivo* biopsies. **(A)** Control sample: the elastic fibers (purple-brown) show a regular distribution throughout the whole dermis. **(B)** Sample harvested after two treatments with 35–40% of the full device working power 1 month after the first treatment: the elastic fibers show a significant thickening throughout the whole dermis; in the papillary dermis the elastic fibers show a more definite perpendicular orientation to the basal membrane (arrows). Light microscopy, orcein staining, bar 180 μm.

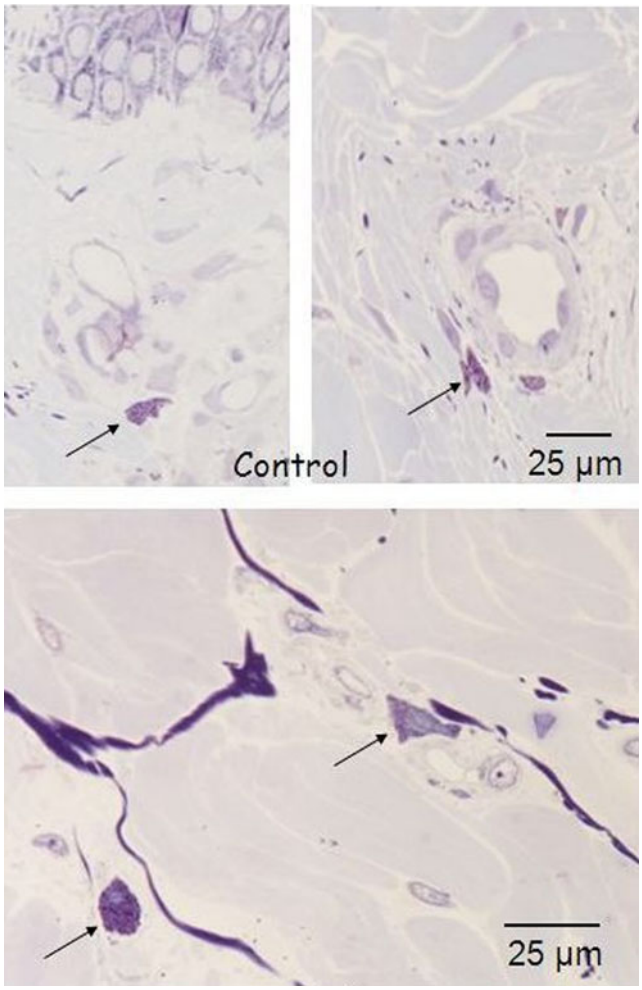

FIG. 28. Histology for macrophages of *in vivo* control biopsy: the arrows highlight the macrophages in quiescent status around the vessels. Light microscopy, toluidine blue staining, bar 25 μm.

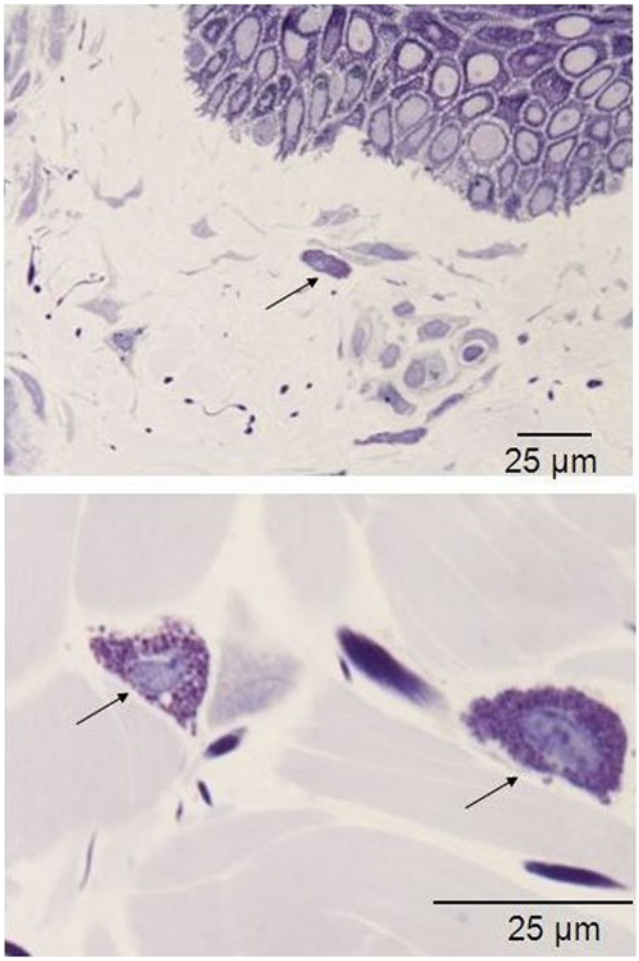

FIG. 29. Histology for macrophages of *in vivo* biopsy harvested after three treatments with 35–40% of the full device working power: the arrows highlight the macrophages that have moved from the perivascular niche, and display a slight increase in their count, thus suggesting an active status. Light microscopy, toluidine blue staining, bar 25 μm.

Acknowledgments

The authors thank Floriana Cazzola and Gian Mario Pelizzoli for their technical support. This work was partially funded by Novavision Group s.p.a., Via dei Guasti 29, 20826 Misinto, Milan, Italy.

Author Disclosure Statement

No competing financial interests exist.

References

1. Beasley, K.L., and Weiss, R.A. (2014). Radiofrequency in cosmetic dermatology. Dermatol. Clin. 32, 79–90.
2. el-Domyati, M., el-Ammawi, T.S., Medhat, W., Moawad, O., Brennan, D., Mahoney, M.G., and Uitto, J. (2011). Radiofrequency facial rejuvenation: evidence-based effect. J. Am. Acad. Dermatol. 64, 524–535.
3. Elsaie, M.L. (2009). Cutaneous remodeling and photorejuvenation using radiofrequency devices. Indian J. Dermatol. 54, 201–205.
4. Zelickson, B.D., Kist, D., Bernstein, E., Brown, D.B., Ksenzenko, S., Burns, J., Kilmer, S., Mehregan, D., and Pope, K. (2004). Histological and ultrastructural evaluation of the effects of a radiofrequency-based nonablative dermal remodeling device: a pilot study. Arch. Dermatol. 140, 204–249.
5. Hantash, B.M., Ubeid, A.A., Chang, H., Kafi, R., and Renton, B. (2009). Bipolar fractional radiofrequency treatment induces neoelastogenesis and neocollagenesis. Lasers Surg. Med. 41, 1–9.
6. Alster, R.S., and Lupton, J.R. (2007). Nonablative cutaneous remodeling using radiofrequency devices. Clin. Dermatol. 25, 487–491.
7. Montesi, G., Calvieri, S., Balzani, A., and Gold, M.H. (2007). Bipolar radiofrequency in the treatment of dermatologic imperfections: clinicopathological and immunohistochemical aspects. J. Drugs. Dermatol. 6, 890–896.
8. Lee, Y.B., Eun, Y.S., Lee, J.H., Cheon, M.S., Cho, B.K., and Park, H.J. (2014). Effects of multipolar radiofrequency and pulsed electromagnetic field treatment in Koreans: case series and survey study. J. Dermatolog. Treat. 25, 310–313.

9. Moritz, A.R., and Henriques, F.C. (1947). Studies of thermal injury II. The relative importance of time and surface temperature in the causation of cutaneous burns. Am. J. Pathol. 23, 695–720.
10. Lin, S.J., Hsiao, C.Y., Sun, Y., Lo, W., Lin, W.C., Jan, G.J., Jee, S.H., and Dong, C.Y. (2005). Monitoring the thermally induced structural transitions of collagen by use of second-harmonic generation microscopy. Opt. Lett. 3, 622–624.
11. Paul, M., Blugerman, G., Kreindel, M., and Mulholland, R.S. (2011). Three-dimensional radiofrequency tissue tightening: a proposed mechanism and applications for body contouring. Aesthetic Plast. Surg. 35, 87–95.
12. Hayashi, K., Thabit, G., Massa, K.L., Bogdanske, J.J., Cooley, A.J., Orwin, J.F., Mark, D., and Markel, M.D. (1997). The effect of thermal heating on the length and histologic properties of the glenohumeral joint capsule. Am. J. Sports Med. 25, 107–112.
13. Willey, A., Kilmer, S., and Newman, J. (2010). Elastometry and clinical results after bipolar radifrequency of skin. Dermatol. Surg. 36, 877–884.

Address correspondence to:
Giovanni Nicoletti
University of Pavia
Salvatore Maugeri Research and Care Institute
Via Salvatore Maugeri, 10
27100 Pavia
Italy

E-mail: giovanni.nicoletti@unipv.it